Mathematical Modeling of Turbine for Optimization of Tidal Energy System

O. S. Oladokun

Alfred-Wegener-Institute, Helmholtz- Centre for Polar and Marine Research, Shelf Sea Ecology Section, Bremerhaven, Germany
Sulaiman.oladokun@awi.de (O.S.O.)
Manuscript received June 3, 2024; accepted July 4, 2024; published July 18, 2024.

Abstract—The oceans of the earth offer vast amounts of renewable energy. Technologies to harness the power of the seas are at an early stage of development. Tidal energy is receiving worldwide attention, as it is a renewable energy that presents high energy density, high predictability, and low environmental impact. This paper presents a theoretical and analysis study of turbines to improve tidal energy systems. The parameter for the structure component that is, the turbine blade is the main component was taken by reading from previous research papers related to the tidal turbine system. In this study, the parameter for structure and hydrodynamic performance, theoretical analysis, and the data of Power Coefficient, Cp is obtained. The maximum Power Coefficient, Cp value for Langkawi, is 0.28 with Tip Speed Ratio, λ 6.26 and 6.43, 0.284 both for Malacca Strait, and Kuala Terengganu with Tip Speed Ratio λ 6.25, 6.31, and 6.41 Cp value with 6.56, 5.94 λ value. The hydrodynamic performance in this research depends on the Power Coefficient, Cp, and Tip Speed Ratio, λ. The most optimum Tip Speed Ratio, λ is the range between 5 and 6. The power output is 0.108 MW can supply electricity to 0.83 houses a year.

***Keywords*—vortex-induced vibrations, numerical simulation, reduced velocity**

I. INTRODUCTION

In general, ocean energy can be divided into six types of different origins and characteristics: ocean wave, tidal range, tidal current, ocean current, ocean thermal energy, and salinity gradient [1, 2]. The most advanced technologies, namely tidal currents and ocean waves still face considerable barriers and many obstacles remain. Research, development, and innovation can help overcome those barriers. Tidal energy is receiving worldwide attention, as it is a renewable form of energy that presents high energy density, high predictability, and low environmental impact. Tidal turbines are interested in a coastal area with reasonable tides. Two types of turbines are usually implied to produce the energy from tides: Horizontal axis and vertical axis. In this study, the turbine of a tidal energy system with a power coefficient of Cp which is the measure of the blade or hydrofoil efficiency. is obtained through theoretical analysis of turbine hydrodynamic performance.

Power coefficient, C_(p) It includes the hydrofoil shape and the hydrodynamic forces of lift and drag. The C_(p) expresses the hydrofoil's ability to transform the water kinetic energy into mechanical power, which is delivered to the turbine transmission or directly to the electrical generator. A higher C_(p) is preferred over a lower C_(p) value. These C_(p) values may vary with the turbine size.

A. Tidal Energy

Tide generation forces lead to the propagation of tidal waves, which can generate strong tidal currents in shelf sea regions. Such regions of strong tidal flow are suitable for electricity generation when intercepted by arrays of tidal energy convertors, but the phase of such electricity generation can vary considerably between shelf sea regions [3–5]. Tidal current energy resources have been assessed for several years. Often, direct measurements have been performed on-site. Recently, 2D and 3D modeling techniques have been applied to determine tidal current energy resources by modeling current velocities. More recent studies assess the hydrodynamic effects of power extraction and consider for example changes to the flow field, changes in water surface elevation, or disturbances in tidal dynamics [6–8]. The tide-generating force is produced by the gravitational attraction between the Earth and the moon and sun, in combination with the rotation of the Earth-moon and Earth-sun systems.

The tide generation due to the moon arises from an imbalance between the forces acting on a particle due to the gravitational attraction of the moon, and the centrifugal force due to the Earth's rotation about the Centre of gravity of the Earth-moon system [9]. Tidal power generation depends on the rise and fall of sea and ocean waters. Terrestrial and celestial gravitational variations predictably affect power generation capacities. Spring tides (high tides) occur on new as well as full moons and neap tides (low tides) occur in waxing or waning half-moons due to misalignment of the earth with the moon and the sun.

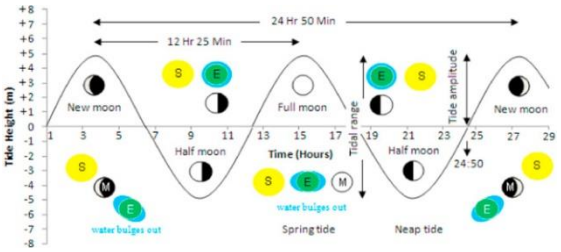

Fig. 1. Natural evolution of spring and neap tides at sea and ocean surfaces [10].

The Earth rotates on its axis at a speed of 16,500 km/h and revolves around the sun at a speed of 107,000 km/y. Earth completes one rotation in one day (24 h) but the moon completes one revolution around the Earth in 29.53 days. A solar month has 30 days in a month, whereas a lunar month has 29 days and 10 min, so the solar month is 50 min longer than a lunar month. In a solar month earth and moon twice become aligned to exert a maximum gravity pull on ocean waters to create spring tides. A range of water springs may be as high as 11.4 m. (Penzhinsk, Russia) to 12.4 m (Cobequid, Canada) Ocean waters bulge out by lunar and solar gravitational forces at the new moon and full moon as

shown in Fig. 1 [11, 12].

Tidal energy can be generated every day and every time from our ocean and it is renewable but we need to do more research and study the field related to the sources and components of the system as well as the impact on biological life and the environment.

B. Turbine

Horizontal or vertical-axis turbines can be used in Fig. 2. Horizontal-axis TSTs can harness energy from a current stream without the requirement to either channelize or impound the flow stream [13]. TSTs generate more power than equivalent-sized wind turbines due to the higher density of water compared with air but consequently, there are greater structural stresses placed on the turbine rotor and supporting structures [14]. The main advantages of Vertical Axis Tidal Turbines (VATT) are the ability to keep the electric generator out of the water, by using floating platforms as support structures, and to be omnidirectional, without the need for any active yaw device. On the other hand, VATT is penalized by low efficiency compared to Horizontal Axis Tidal Turbines (HATT) and by self-starting issues. Then, it is essential to increase the efficiency of the overall arrangement as well as the power density. To increase the power produced in a given area of the sea it would be convenient to place a farm of high Aspect-Ratio (AR> 2) turbines arranged as close as possible, compatibly with the negative effects of wake interactions. Numerical studies aimed to optimize the arrangement of HATT or VATT farms or rows proved that the local blockage mechanism (the acceleration of flow between two adjacent turbines) can be exploited to increase energy production by dislocating the turbines belonging to two consecutive rows in a staggered [15, 16].

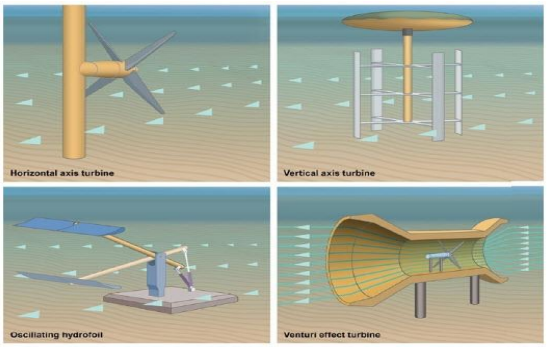

Fig. 2. Primary types of tidal flow energy conversion devices.

Two kinds of flow energy conversion technologies, namely oscillating hydrofoils or airfoils systems and vortex-induced vibration systems are possible [17]. The concept of using oscillating foil to harvest energy from fluid was first tested by [18]. The application of oscillating wings for energy extraction is inspired by the biological ability of animals, such as aquatic animals and birds, who exhibit excellent hydrodynamic and aerodynamic performance by extracting flow energy through their wing and tail fin's flapping motion [19].

Many types of turbines can be used to harvest tidal energy such as horizontal axis turbines, vertical axis turbines, oscillating hydrofoils, and venture effect turbines.

C. Environment

The coastal environment influences the hydrodynamics process such as waves, currents, wind, and others. All of these factors are linked to the tidal energy that comes from the ocean.

Coastal areas with a higher energetic level, for a given geological setting, will experience a higher degree of mobility and therefore vulnerability, considering that human uses and infrastructures tend to be static. Yet coastal environments subject to a higher level of incoming energy are more naturally prepared to deal with climatic variability or change [20]. However, tidal energy development and marine current turbine deployment face some important issues. One of the main issues is the tidal systems' optimal location as suitable tidal sites are limited. Indeed, tidal turbines cannot be installed in shallow waters due to the turbulence caused by waves [21]. Otherwise, they cannot also be placed in deep waters due to the decrease in the current velocity with the depth; as well as for the high costs induced by deep ocean projects. In addition to these issues, it should also be mentioned that tidal systems technology is not as mature as wind turbines or PV systems [22].

D. Computational Fluid Dynamics (CFD)

Computational Fluid Dynamics (CFD) is a tool or way that is used to do simulation and prediction of fluid flows by mathematical modeling, numerical modeling, and software tools. Laboratory experiments cannot truly mimic complex offshore conditions; they are very convenient due to significantly lower costs compared to offshore deployments. Laboratory experiments provide a platform for collecting accurate and repeatable data. In contrast, Computational Fluid Dynamics (CFD) modeling has the potential to simulate the effect on environmental conditions at a significantly lower cost compared to offshore deployments [23]. Fig. 3 shows the partial flow field.

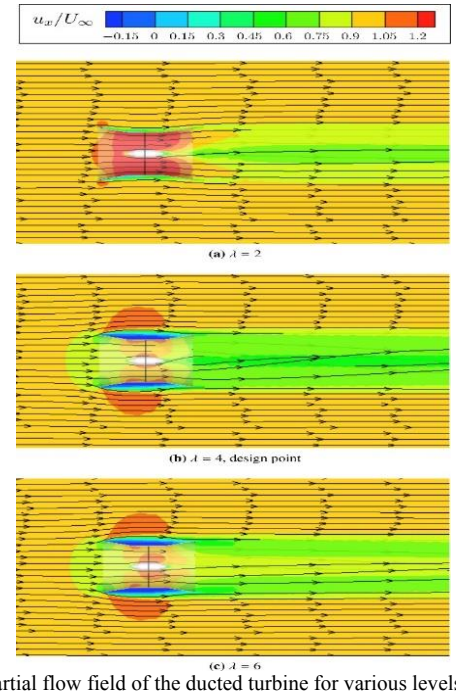

Fig. 3. Partial flow field of the ducted turbine for various levels of λ [24].

E. Hydrodynamic Performance

The hydrodynamic analysis of the horizontal-axis turbine

in a wave-current field is very complicated, and it is difficult to use CFD software to simulate the wave-current field directly. Hence, we simplify the hydrodynamic problems of the horizontal-axis turbine with multi-degree freedom wave-induced movements and put forward the following two assumptions: 1) the turbine is fixed on a floating carrier with a main shaft, and the floating carrier has a slightly simple harmonic motion with wave action; and 2) the inflow velocity is a constant with no influence of waves, which means that we assume that the tip-immersion depth is deep enough. Based on these assumptions, the hydrodynamic problems of the horizontal-axis turbine with wave motion can be simplified as problems of a turbine with multi-degree of freedom simple harmonic motion in a constant tidal current [25, 26]. The meshing of the turbine is shown in Fig. 4. The computational domain requires discretization when it is built, namely, meshing. Meshing is a very important element of the numerical simulation technique as the grid quality directly affects the accuracy and efficiency of the numerical calculation. The meshing of the entire computational domain adopts the methods of structured grid and unstructured grid. Because the shape of the rotation domain for the turbine is complex, it is difficult to achieve a high-quality structured grid without simplifying the model. Therefore, it is better to adopt an unstructured grid; the rolling, surging, deformation, and static domains have regulation shapes, so adopting a structured grid is beneficial to improving the calculation efficiency [27, 28].

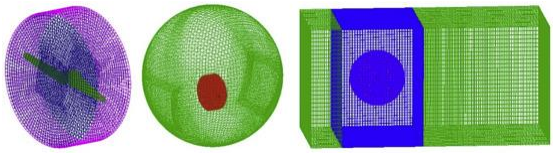

Fig. 4. Grid model of rotation, rolling, and surging coupled motion.

II. METHODOLOGY

This section shows how this research has been conducted. First, the study of parameters for the performance of structure and hydrodynamic, parameters for the structure component that is turbine blade that is the main component was taken by reading from previous research paper that related to the tidal turbine system. Second, design geometry of the system model using the drafting software, AutoCAD. Third, the theoretical analysis is determined by referring to the previous research paper. A suitable equation and formula are used to calculate the power coefficient, C_p and Thrust Coefficient, C_T. Lastly, compare the hydrodynamic performances (Fig. 5).

A. Study of Parameter for the Performance of Structure and Hydrodynamic

The parameter for the structural component of the turbine blade that represents the main component was taken by reading from a previous research paper that related to the tidal turbine system. The turbine blade that is used in this project is the two-blade turbine and also the three-blade turbine with pitch angles of 0^0 and $5^{0.}$ For hydrodynamic performance, the important parameters are the Tip Speed Ratio, TSR, and the power coefficient, Cp. The TSR is the ratio between the tangential speed of the tip of the blade with the actual speed of the wind, and in this study, the wind is changed with water (See Tables 1 and 2). The tip speed ratio and the power coefficient, Cp need to be calculated by using the equation referenced from a selected research paper.

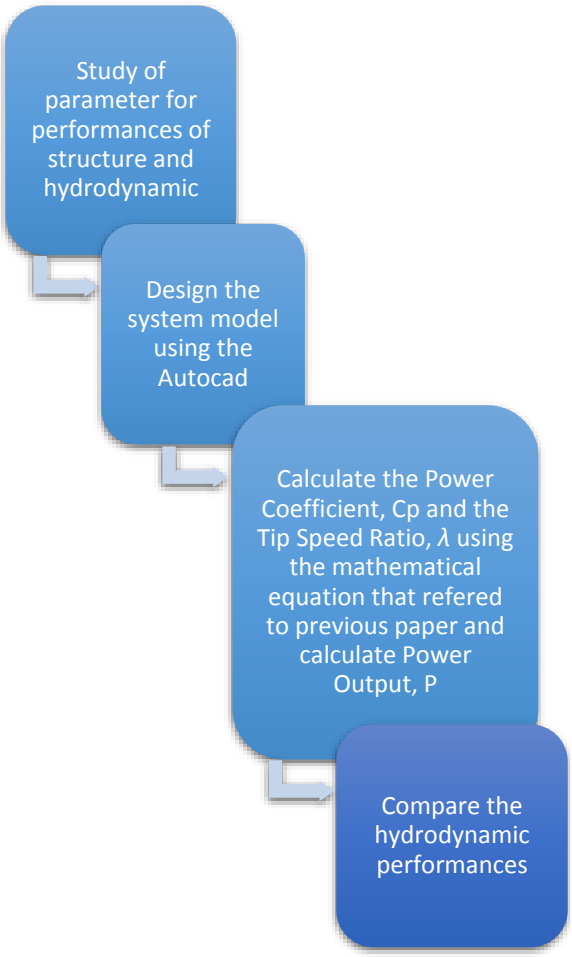

Fig. 5. Methodology flow chart.

Parameter of the turbine

Table 1. Parameter of the turbine

Turbine	Number of blades	Pitch angle	Rotor radius
A	2	0°, 5°, 10°	5 m
B	3	0°, 5°, 10°	5 m

Material properties of the turbine

Material type: Grade 446 stainless steel

Table 2. Material properties

Density	Young's Modulus	Poisson Ratio	Tensile Strength
7800 kg/m^3	200 GPa	0.30	550 MPa

Water properties

Salt Water

Table 3. Water properties

Density	Viscosity	Water Velocity
1028 kg/m^3	0.00188 Ns/m^2	2.5 m/s

B. Geometry Model

AutoCAD software is used for the design and drafting of the 2D and 3D models, the whole tidal turbine system is designed by using AutoCAD. The design of the turbine blade which is the main component uses a set of airfoils that have different shapes and sizes. Airfoil which is the cross-sectional shape of the blade is arranged in a straight line that uses the loft command in AutoCAD to create the blade model (Fig. 6).

1) System Model

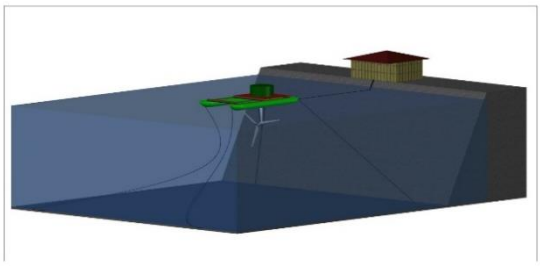

Fig. 6. A system model.

2) Model Design

Table 4. Dimension of the model

Length	Width	Overall height	Rotor Diameter
8.80 Meter	5.50 Meter	7.73 Meter	5 Meter

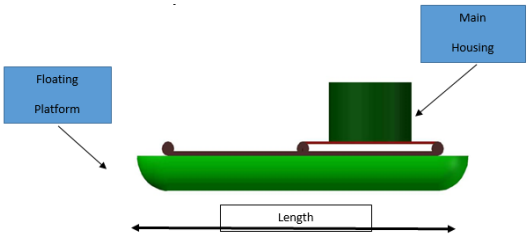

Fig. 7. System model.

This model consists of several parts such as a floating platform, main housing, secondary housing, turbine blade, hub, model frame, and pylon (Fig. 7). The floating platform keeps the main housing and the model frames the sea level (Fig. 8). The main housing places the circuit breaker that helps protect all the instruments from short circuits due to excess current and a connector that connects the cable to the power station.

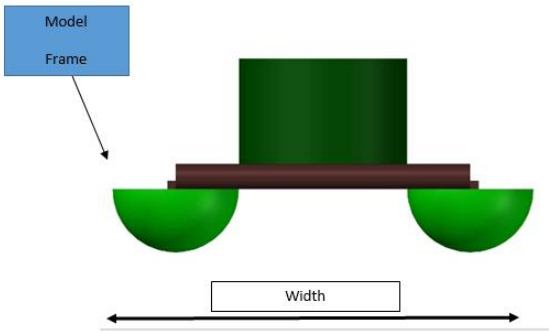

Fig. 8. System model.

The model frame is made of stainless steel, which slows the rate of corrosion (Fig. 9). For the structure to last longer than the use of normal steel. The pylon or pillar-like structure carries the cable from the secondary housing below (Fig. 10). The secondary sing, in this part, stores important components generator, main gearbox, drive shaft, and high-speed shaft.

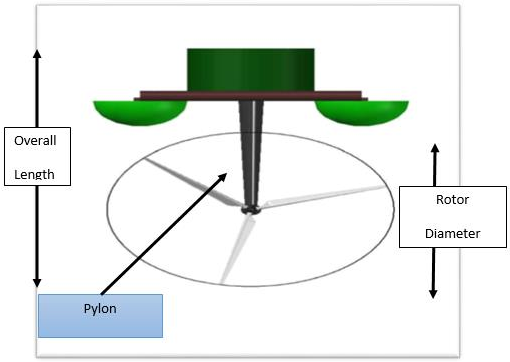

Fig. 9. System model.

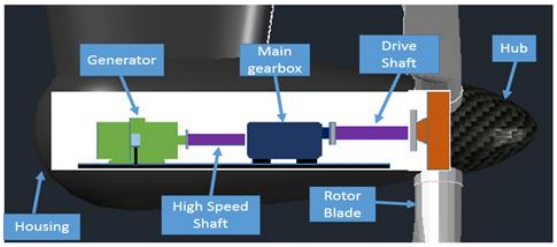

Fig. 10. Component in the secondary housing.

C. Theoretical Analysis

In this study, the theoretical analysis is determined by referring to the previous research paper.

The equations are used to calculate the power coefficient, C_p and Thrust Coefficient, C_T.

1) Power Coefficient, C_p

The performance of a hydrokinetic turbine is the main concern. It depends on the interaction between the rotor and the water current. The rotor is an important component in a turbine, which must be designed for capturing water energy and converting it into rotating mechanical energy. The rotor consists of several blades joined to a common hub.

The turbine blades are critical components of the rotor, which use the flow to cause a pressure difference on either side of the hydrofoil profile, creating a resultant force on the blade profile and, subsequently, causing a rotational movement. This rotating movement of the rotor shaft is passed, in most cases, through a gearbox to increase the number of revolutions of the moving rotor. The output of the gearbox is directly coupled to a generator, which is used to produce electricity and transfer it to the desired location via cables. For this purpose, to find the performance of the turbine, it is widely known that the energy in moving water is in the form of kinetic energy, which may be expressed using Eq. (1):

$$E = \frac{1}{2} mV_1^2 \quad (1)$$

where m and V_1 correspond to the mass and the velocity of the object, respectively. In a hydrokinetic turbine, there are several units of water masses moving perpendicularly to the plane or Area (A) swept out by the blades. This area can be expressed as $A = \pi R^2$, where R is the blade radius. In turn, the Power (P) is the rate of energy movement per unit of time or the rate at which energy is generated or consumed per unit of

time. Mathematically, *P* is the first derivative of the energy taken concerning time (*dE/dt)*. This power is developed in the hydrokinetic turbine from the mass movement of water, as indicated in Eq. (2):

$$P = \frac{dE}{dt} = \frac{1}{2}\frac{dm}{dt}V^2 \quad (2)$$

The next step is to quantify the amount of water flow associated with *dm/dt*. Given a unit of time (*t*), the unit of water masses (*m*) is moved at a distance of *L*. This can be used to arrive at two important results. First, the first derivative of *L* with respect to *t* is *dL/dt*, which is equal to velocity (*V*1). Second, the volume of water passing through *A* will be *AL*. If the density of water (ρ) is known or can be found, then the mass of water moving through plane *A* is $m = \rho AL$. The mass movement rate *dm*/*dt* is equal to $\rho AdL/dt$ or the expression represented in Eq. (3):

$$\frac{dm}{dt} = \rho AV^2 \quad (3)$$

Substituting Eq. (3) into Eq. (2), Eq. (4) is obtained:

$$P = \frac{1}{2}\rho AV^3 \quad (4)$$

Eq. (4) expresses the ideal power in a fluid flow. However, hydrokinetic turbines are limited by blade efficiencies, mechanical losses in transmissions, electrical losses, and the theoretical amount of energy allowed to be extracted from the water current. Because of these losses and inefficiencies, two more variables must be added to Eq. (4).

The first variable is η, which is a measure of the efficiency of the gearbox, the electrical inverter, and the generator. This variable takes into account all the friction, slippage, and heat losses associated with the internal mechanical and electrical components. Values of η may greatly differ among the different turbine models. A reasonable and conservative value of η can be around 70%. The second variable is the power coefficient (*Cp*), which refers to a measure of the blade or hydrofoil efficiency. It includes the hydrofoil shape and the hydrodynamic forces of lift and drag. The *Cp* expresses the hydrofoil's ability to transform the water kinetic energy into mechanical power, which is delivered to the turbine transmission or directly to the electrical generator. A higher *Cp* is preferred over a lower *Cp* value. These *Cp* values may vary with the turbine size. Placing these two variables, η and *Cp*, into Eq. (4), the following expression is obtained:

$$P = \frac{1}{2}\rho AV^3 C_p \eta \quad (5)$$

Eq. (5) is considered to determine the power of the hydrokinetic turbine. *P* is the net power derived from the water after accounting for losses and inefficiencies. From this equation, it can be seen that the extractable power is dependent on the turbine power coefficient, the density of the flow medium, the swept area of the turbine, and the mean velocity of water (*V*1). If the water density, blade radius, and water velocity are constant, the captured power (*P*) is proportional to the *Cp*, which depends on the Tip-Speed Ratio (TSR) (λ) and the pitch angle of the turbine (θ), as in wind turbines. The maximization of *Cp* is of fundamental importance to optimize the extraction of energy from water. It is highlighted that λ is the ratio between the speed of the blade at its tip and the speed of the water current. This ratio has a strong influence on the efficiency of the turbine. This variable may be defined as Eq. (6):

$$\lambda = \frac{R\omega}{V} \quad (6)$$

where ω is the rotational speed of the rotor of the hydrokinetic turbine (rad/s). The calculation of the *Cp* requires the use of the blade element theory. However, numerical approximations have been developed [11]. In the current work, Eq. (7) was used:

$$end\ C_p(\lambda,\theta) = 0.22\left(\frac{116}{\lambda} - 0.4\theta - 5\right)e^{\frac{-12.5}{\lambda}} \quad (7)$$

$$\frac{1}{\lambda} = \frac{1}{\lambda + 0.8\theta} - \frac{0.035}{\theta^3 + 1} \quad (8)$$

With the function defined in Eq. (8), it is possible to evaluate *Cp* at different values of tip-speed ratio and pitch angle. This leads to the *Cp* (λ, θ) versus λ characteristics for various values of θ *[2].*

D. Compare the Hydrodynamic Performances

Data from the theoretical analysis of the Power Coefficient, C_p and Tip Speed Ratio, λ is compared. The angular velocity speed, ω that is calculated will be inserted into the equation and formula to find the power coefficient, C_p. The graph of the Tip Speed Ratio against the Power Coefficient C_p is plotted. From this graph, the result of the hydrodynamic performance of the turbine is obtained.

III. Result and Discussion

In this paper, the result obtained through the theoretical analysis which uses the equation to estimate the Power Coefficient, C_p and Tip Speed Ratio, λ as stated in the methodology. However, the data of the current velocity that is retrieved from the source is very small and the result obtained is not compatible with the reference research paper. To obtain a good result, the current velocity data is magnified by a ratio of 1:10 and the period, T is assumed to be 1 rotation per second.

The value is used to evaluate the Power Coefficient, C_p at different values of Tip Speed Ratio, λ, and pitch angle. The pitch angle values used in this analysis are 0^0, 5^0, and 10^0, the current velocity data that is also included in this analysis is characterized according to different locations that are Langkawi (97.8E–99.8E, 6.2N–8.2N), Malacca Strait

(99.8E–101.8E, 4.2N–6.2N) and Kuala Terengganu (101.8E–103.8E, 4.2N–6.2N).

A. Langkawi

The value for Power Coefficient, *Cp* obtained at pitch angles 0^0, 5^0, and 10^0 is shown in Fig. 11. At pitch angle 0^0, the value of Power Coefficient, *Cp* starts at 0.26 with a Tip Speed Ratio of 5.08. Slightly increase to 0.28 of Cp at λ 6.26 and 6.43. Then The Cp value decreases to −0.16 at λ 15.7. From this graph, the highest value of the Power Coefficient, Cp is 0.28 for pitch angle 0^0. For pitch angle 5^0, The Cp value starts at 0.27 with λ 5.08, increases to 0.284 with λ 5.8 then the Cp value decreases to −0.18 at λ 15.7. After that, for pitch angle 10^0 the Cp value starts at 0.281 with λ value at 5.08. The Cp value then slightly increases to a maximum of 0.284 with λ 5.59. Then the Cp value decreases to −0.2 with λ 15.7.

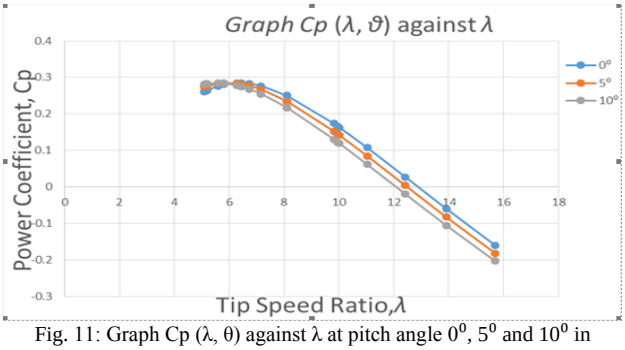

Fig. 11: Graph Cp (λ, θ) against λ at pitch angle 0^0, 5^0 and 10^0 in Langkawi.

B. Malacca Strait

The Power Coefficient, Cp from Fig. 12 show that for pitch angle 0^0 starts at 0.019, for 5^0 starts at 0.04, and for 10^0 start at 0.07 with the same Tip Speed Ratio value that is 1.97. Then, the Cp value increases to maximum value of 0.284 at λ 6.25, 6.31, and 6.41. Lastly, the Cp decreased to 0.165 for pitch angle 0^0, 0.144 for pitch angle 5^0, and 0.122 for pitch angle 10^0 at λ value 9.96.

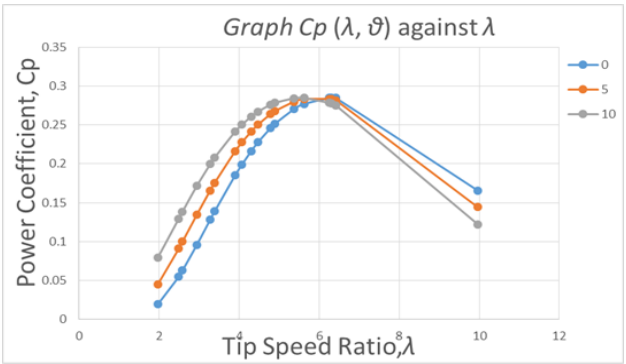

Fig. 12. Graph Cp (λ, θ) against λ at pitch angle 0^0, 5^0, and 10^0 in Malacca Strait.

C. Kuala Terengganu

The Power Coefficient, Cp from Fig. 13 shows that for pitch angle 0^0 starts at 0.166, for 5^0 start at 0.199, and for 10^0 starts at 0.228 with the same Tip Speed Ratio value that is 3.68. Then, the Cp value increases to a maximum value of 0.284 at λ 6.56, 5.94, and a Cp value of 0.283 at λ 5.21. Lastly, the Cp value decreases to −0.44 for pitch angle 0^0, −0.45 for pitch angle 5^0, and −0.47 for pitch angle 10^0 at λ value 9.96.

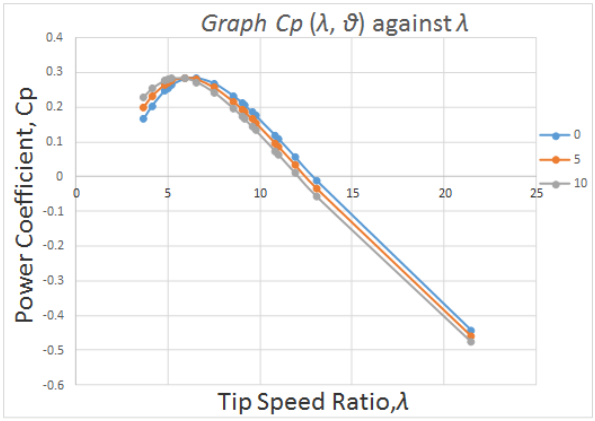

Fig. 13: Graph Cp (λ, θ) against λ at pitch angles 0^0, 5^0, and 10^0 in Kuala Terengganu.

D. Output Power

The output power, P for this turbine is calculated using Eq. (9),

$$P = \frac{1}{2}\rho A V^3 C_p \eta \quad (9)$$

With a rotor diameter of 5 Meters, Power coefficient, Cp 5.015974, current velocity 0of .314 m/sdensity of water is 1028 $kg/m^3$and the efficiencies η, which is a measure of the efficiency of the gearbox, the electrical inverter, and the generator. This variable takes into account all the friction, slippage, and heat losses associated with the internal mechanical and electrical components. Values of η may greatly differ among the different turbine models. A reasonable and conservative value of η can be around 70 %. The power output of this turbine is 0.108 MW, which is compatible and from this equation, the turbine power output is influenced by power coefficient Cp, the density of water ρ, swept area of turbine Aelocity of water, V.

IV. Conclusion

In this study, the parameter for structure and hydrodynamic performance, theoretical analysis, and the data of Power Coefficient, Cp is obtained. The maximum Power Coefficient, Cp value for Langkawi is 0.28 with a Tip Speed Ratio, of λ 6.26 and 6.43, 0.284 both for Malacca Strait, and Kuala Terengganu with a Tip Speed Ratio λ 6.25, 6.31, and 6.41 Cp value with 6.56, 5.94 λ value. The hydrodynamic performance in this research depends on the Power Coefficient, Cp and Tip Speed Ratio, λ. The most optimum Tip Speed Ratio, λ is the range between 6. The power output is 0.108 MW can supply electricity to 0.83 houses a year.

Further work has to be done in the field related to this energy. This finding is still not enough because this is only a theoretical analysis. To obtain a good and very compatible result, experimental and numerical investigation need to be done.

Conflict of Interest

The author declares no conflict of interest.

ACKNOWLEDGMENTS

Acknowledgment to Muhamad Fuad for his direct contribution to the study

REFERENCES

[1] A. Uihlein and D. Magagna, "Wave and tidal current energy—A review of the current state of research beyond technology," *Renewable and Sustainable Energy Reviews*, vol. 58, pp. 1070−1081, 2016.

[2] C. M. Johnstone *et al.*, "A techno-economic analysis of tidal energy technology," *Renewable Energy*, vol. 49, pp. 101−106, 2013.

[3] S. P. Neill *et al.*, "Tidal energy leasing and tidal phasing," *Renewable Energy*, vol. 85, pp. 580−587, 2016.

[4] R. Bedard. (February 2022). Overview: EPRI ocean energy program. *Presented to Duke University Global Change Center* [Online]. Available: http://oceanenergy.epri.com/attachments/ocean/briefing/Duke_Sep_14.pdf

[5] O. O. Sulaiman *et al.*, "Review on potential for waste recycled based bioenergy for the marine system," *Int. Journal Environmental Technology and Management (IJETM) Inderscience*, vol. 14, pp. 339−357, 2011.

[6] S. Serhadlıoğlu *et al.*, "Tidal Stream Energy resource assessment of the Anglesey Skerries," *International Journal of Marine Energy*, vol. 3, e98-e111, 2013.

[7] S. O. Oladokun, K. F. Tee, and A. S. A. Kader, "Water quality test and site selection for suitable species for seaweed farm on the east coast of Malaysia," *Biosci. Biotech. Res. Asia*, pp. 33−39, 2015.

[8] S. O. Oladokun, A. H. Saharuddin, and A. S. A. Kader, "Modelling of gas turbine co-propulsion engine to ecotourism vessel to improved sailing speed up to 35 Knots," *International Journal of Engineering*, vol. 4, no. 6, pp. 463−477, 2011

[9] R. M. Cavin, "Introduction to the physical and biological oceanography of shelf seas, John H. Simpson, Jonathan Sharples. Cambridge University Press, Cambridge, and New York, 2012," *Geomorphology (Amsterdam)*, vol. 204, pp. 692−693, 2014.

[10] N. D. Khan *et al.*, "Review of ocean tidal, wave, and thermal energy technologies," *Renewable and Sustainable Energy Reviews*, no. 72, pp. 590−604, 2017. doi: 10.1016/j.rser.2017.01.079

[11] S. O. Oladokun and A. S. A. Kader, "Solar-macro-algae-based biogas hybrid system for future offshore installation," *Biosciences Biotechnology Research Asia*, vol. 10, no. 2, pp. 53−61, 2013.

[12] G. S. Payne *et al.*, "Design and manufacture of a bed-supported tidal turbine model for blade and shaft load measurement in turbulent flow and waves," *Renewable Energy*, vol. 107, pp. 312−326, 2017.

[13] M. J. Khan *et al.*, "Hydrokinetic energy conversion systems and assessment of horizontal and vertical axis turbines for river and tidal applications: A technology status review," *Applied Energy*, vol. 86, no. 10, pp. 1823−1835, 2009.

[14] A. S. Bahaj *et al.*, "Power and thrust measurements of marine current turbines under various hydrodynamic flow conditions in a cavitation tunnel and a towing tank," *Renewable Energy*, vol. 32, no. 3, pp. 407−426, 2007.

[15] M. G. Gebreslassie *et al.*, "Investigation of the performance of a staggered configuration of tidal turbines using CFD," *Renewable Energy*, vol. 80, pp. 690−698, 2015.

[16] E. Chica and A. Rubio-Clemente, "Renewable hydropower technologies," in *Design of Zero Head Turbines for Power Generation*, B.I. Ismail, Ed. London, UK: IntechOpen, 2017, ch. 03.

[17] W. Jiang *et al.*, "Numerical investigation into the effects of arm motion and camber on a self-induced oscillating hydrofoil," *Energy*, vol. 115, pp. 1010−1021, 2016.

[18] W. McKinney and J. DeLaurier, "Windmill: An oscillating-wing windmill," *Journal of Energy*, vol. 5, no. 2, pp. 109−115, 1981.

[19] K. Lu *et al.*, "Nonsinusoidal motion effects on energy extraction performance of a flapping foil," *Renewable Energy*, vol. 64, pp. 283−293, 2014.

[20] A. Sánchez-Arcilla *et al.*, "Managing coastal environments under climate change: Adaptation pathways," *Science of The Total Environment*, vol. 572, pp. 1336−1352, 2016.

[21] Z. Zhou *et al.*, "Power control of a nonpitchable PMSG-based marine current turbine at overrated current speed with flux-weakening strategy," *IEEE Journal of Oceanic Engineering*, vol. 40, no. 3, pp. 536−545, 2015.

[22] A. S. Bahaj, "Generating electricity from the oceans," *Renewable and Sustainable Energy Reviews*, vol. 15, no. 7, pp. 3399−3416, 2011.

[23] M. Edmunds *et al.*, "An enhanced disk averaged CFD model for the simulation of horizontal axis tidal turbines," *Renewable Energy*, vol. 101, pp. 67−81, 2017.

[24] C. S. K. Belloni *et al.*, "An investigation of ducted and open-center tidal turbines employing CFD-embedded BEM," *Renewable Energy*, vol. 108, pp. 622−634, 2017.

[25] S.-q. Wang *et al.*, "Hydrodynamic analysis of horizontal-axis tidal current turbine with rolling and surging coupled motions," *Renewable Energy*, vol. 102, pp. 87−97, 2017.

[26] J. Yan *et al.*, "Free-surface flow modeling and simulation of horizontal-axis tidal-stream turbines," *Computers and Fluids*, vol. 158, pp. 157−166, 2017.

[27] S. O. Oladokun, "Solar hybrid power system for marine diesel engine: UMT vessel experience," in *Marine Technology and Sustainable Development*, IGI Publisher, 2013, pp. 1−8.

[28] H. T. Pham *et al.*, "Performance comparison of sensor fault-tolerant control strategies for PMSG-based marine current energy converters," in *Proc. IECON 2015—41st Annual Conference of the IEEE Industrial Electronics Society*, 2015.

Copyright © 2024 by the authors. This is an open-access article distributed under the Creative Commons Attribution License which permits unrestricted use, distribution, and reproduction in any medium, provided the original work is properly cited (CC BY 4.0).